DALTON
FULL PAPER

Theoretical study of the geometric and electronic structures of pseudo-octahedral d^0 imido compounds of titanium: the *trans* influence in *mer*-$[Ti(NR)Cl_2(NH_3)_3]$ (R = Bu^t, C_6H_5 or $C_6H_4NO_2$-4)

Nikolas Kaltsoyannis [a] **and Philip Mountford** [b]

[a] *Centre for Theoretical and Computational Chemistry, University College London, 20 Gordon Street, London, UK WC1H 0AJ. E-mail: n.kaltsoyannis@ucl.ac.uk; web: http://calcium.chem.ucl.ac.uk/webstuff/people/nkalt/index.html*
[b] *Inorganic Chemistry Laboratory, South Parks Road, Oxford, UK OX1 3QR. E-mail: philip.mountford@chemistry.oxford.ac.uk; web: http://www.chem.ox.ac.uk/researchguide/pmountford.html*

Received 14th September 1998, Accepted 20th January 1999

The geometric and electronic structure of *mer*-$[Ti(NR)Cl_2(NH_3)_3]$ (R = Bu^t, C_6H_5 or $C_6H_4NO_2$-4), models for the corresponding crystallographically characterised pyridine complexes $[Ti(NR)Cl_2(py)_3]$, have been studied computationally using non-local density functional theory. In general, excellent agreement is found between the fully optimised calculated geometries and the experimental structures. Each of the molecules is calculated to have a significantly longer Ti–NH_3 (*trans*) distance than Ti–NH_3 (*cis*), this *trans* influence decreasing in the order $Bu^t > C_6H_5 > C_6H_4NO_2$-4. This result supplements the crystallographic results, which found no experimentally significant difference in the *trans* influences in $[Ti(NR)Cl_2(py)_3]$ (R = Bu^t, C_6H_5 or $C_6H_4NO_2$-4). The causes of the *trans* influence have been investigated. Approximately 25% of the *trans* influence in the fully optimised geometries arises from π orbital driven increases in the RN≡Ti–Cl angle, which lead to increased steric repulsion between the *cis* Cl atoms and the *trans* NH_3 group. This contrasts sharply with the situation for $[OsNCl_5]^{2-}$ (studied previously by other workers and revisited in the present contribution) in which most of the *trans* influence depends on *cis*–*trans*-Cl ligand repulsions as the N≡Os–Cl (*cis*) angles relax from 90° to their fully optimised value. The remaining 75% of the *trans* influence for the title titanium imides is attributed to their intrinsic electronic structures, and in particular to two occupied molecular orbitals which are Ti–NH_3 (*trans*) antibonding and which vary in composition according to the identity of the imido N-substituent. By contrast, none of the molecules has an occupied orbital which is Ti–NH_3 (*cis*) antibonding.

Introduction

The *trans* influence, the tendency of a ligand to weaken the bond *trans* to itself, is a well established phenomenon in transition metal chemistry that has received a great deal of both experimental and theoretical study.[1–8] It has been suggested that the *trans* influence is electronic in origin, in that two ligands are forced to compete for the same metal orbital(s), resulting in a relative weakening of one of the metal–ligand bonds. Steric arguments have also been put forward to explain the *trans* influence, in which a bond angle of greater than 90° between one of the two mutually *trans* ligands and the *cis* groups in a pseudo-octahedral complex leads to increased steric repulsion between the *cis* groups and the other *trans* ligand, and hence to a lengthening of the bond between that ligand and the metal centre. The *trans* influence can be particularly strong when one of the *trans* ligands is multiply bonded to the metal, for example in systems containing nitrido, oxo or imido moieties, which almost invariably possess E≡M–L(*cis*) (E = N, O, NR; M = transition metal) angles greater than 90°.[1,9]

As part of our on-going studies of Ti imido chemistry [10–14] we have reported the synthesis, structural characterisation and imido group exchange reactions of pseudo-octahedral $[Ti(NR)Cl_2(py)_3]$ (R = Bu^t, C_6H_5, 4-C_6H_4Me or $C_6H_4NO_2$-4).[7,8] These compounds are particularly interesting because they form the first structurally characterised homologous series in which only the R substituent on the imido N atom is modified, permitting us to evaluate directly the structural effects of the variations in R on the rest of the molecule. This is an important feature since the reactivity and properties of imido complexes in general are substantially influenced by the identity of the imido N-substituent.[1,9] X-Ray crystallography revealed that in all cases the NR ligands exert a significant *trans* influence. Most interestingly, if we define the term 'structural influence' to be the extent to which a given imido ligand perturbs *all* of the geometric parameters within the molecule (as distinct from the *trans* influence which, by definition, is the specific difference between the Ti–py (*trans*) and Ti–py (*cis*) bond lengths) then our X-ray crystallographic data indicated that while there are appreciable differences between the structural influences of the various NR ligands, there are no experimentally significant differences in the *trans* influences. In this contribution we report the results of a computational investigation of the geometric and electronic structures of $[Ti(NR)Cl_2(NH_3)_3]$ (R = Bu^t, C_6H_5 or $C_6H_4NO_2$-4), models for the pyridine containing molecules. The aim of this study is twofold; to establish the origin of the *trans* influence in these compounds and to probe further the experimental observation of different structural influences but experimentally indistinguishable *trans* influences.

Computational and theoretical details

A General

Calculations were performed with the Amsterdam Density Functional (ADF) program suite.[15,16] ADF Type IV basis sets

were used for the Ti calculations, *i.e.* uncontracted triple-zeta Slater-type valence orbitals supplemented with a p polarisation function for H and a d function for C, N, O and Cl. No polarisation functions were included for Ti. Non-relativistic frozen cores were employed for C (1s), N (1s), O (1s), Cl (2p) and Ti (2p). For the Os calculations, quasi-relativistic[17] frozen cores were used for N (1s), Cl (2p) and Os (4f), together with ADF Type IV valence functions. Relativistic core potentials were computed using the ADF auxiliary programme 'Dirac'. The density functional of Vosko, Wilk and Nusair[18] was employed in all calculations, in conjunction with Becke's gradient correction[19] to the exchange part of the potential and the correlation correction due to Perdew.[20] Mulliken population analyses were performed.[21] Unless otherwise indicated, molecular geometries were fully optimised with no symmetry restrictions, and confirmed as true energy minima by the observation of only positive eigenvalues in the Hessian matrices and hence no imaginary vibrational wavenumbers.

Molecular orbital plots were generated using the program MOLDEN, written by G. Schaftenaar of the CAOS/CAMM Centre, Nijmegen, The Netherlands. The ADF output files (TAPE21) were converted to MOLDEN format using the program ADFrom written by F. Mariotti of the University of Florence.[22] The calculations were performed on IBM RS/6000 and DEC 433au workstations and the EPSRC's 'Columbus/Magellan' computer.

B Energy decomposition scheme

The terms 'electronic effect' and 'steric effect' are often used by inorganic chemists to rationalise molecular structure, bonding and reactivity, though the precise definition of electronic and steric is in many cases unclear. ADF includes an energy decomposition scheme in which the electronic and steric contributions to the total molecular bonding energy have rigorous, explicit definitions. As we shall make use of this scheme in this article, it is important that we set out exactly what we mean by 'electronic' and 'steric'.

The energy decomposition scheme employed within ADF is based on the generalised transition state method developed by Ziegler and Rauk.[23,24] The total molecular bonding energy is defined as the energy difference between the molecular fragments in their final positions and at infinite separation. These molecular fragments may be individual atoms or groups of atoms, though in our study only atomic fragments are considered.† These fragments are placed at their positions within the molecule. At this point there is an electrostatic interaction between them, comprising the nucleus/nucleus, nucleus/electron and electron/electron Coulombic interactions. Next we ensure that the overall molecular wavefunction satisfies the Pauli principle. We do this by requiring that the one-electron orbitals of the combined fragments form a correct single-determinantal wavefunction. It is extremely unlikely, however, that this will be the case for the fragment orbitals when the fragments are simply placed at their positions within the molecule because the orbitals on the different fragments will not be orthogonal to one another. Thus the next step is to orthogonalise the occupied fragment orbitals to obtain a correct single-determinantal, antisymmetrised molecular wavefunction. This will result in a change in the molecular charge density, and the accompanying energy change is known as the Pauli repulsion. The steric interaction is defined as the combination of the electrostatic interaction and the Pauli repulsion, and may be thought of as the energy of interaction between the fragments when none of the fragments can change in response to the presence of the others and no electron transfer can take place. The final part of the process is to allow the fragment orbitals to relax to self-consistency. This interaction energy between the orbitals of the various fragments is defined as the electronic (or orbital) interaction.

† For a discussion of the use of atomic fragments in density functional calculations, see ref. 25.

Results and discussion

A Geometric structures of $[Ti(NR)Cl_2(NH_3)_3]$ (R = Bu^t, C_6H_5 or $C_6H_4NO_2$-4)

Table 1 presents selected bond lengths and angles from the fully optimised geometries of the title model compounds. Also summarised are the X-ray crystallographic data[7,8] previously reported for the real compounds in which the NH_3 ligands are replaced by pyridine groups.‡ It may be seen that the agreement between experiment and theory is excellent, the *largest* discrepancy in the bond lengths being 0.027 Å in the averaged Ti–N (*cis*) distances for $[Ti(NC_6H_5)Cl_2(NH_3)_3]$. The slight lengthening of the calculated Ti–N(ammonia) single bond distances in general, compared to the experimental Ti–N(pyridine) bond distances, probably reflects the different donor abilities of the two types of ligand. The difference between the calculated and experimental bond angles is also small, 4° or less for R = Bu^t and C_6H_5 and slightly more for R = $C_6H_4NO_2$-4. In all cases the calculations underestimate the N≡Ti–N (*cis*)§ angles and overestimate the N≡Ti–Cl (*cis*) angles. Given the relative sizes of NH_3 and py and the consequent differences in their steric influence, this result is entirely acceptable.

The trend in the calculated Ti≡NR distances is the same as that found experimentally, with an increase from R = Bu^t to $C_6H_4NO_2$-4. By contrast, the Ti–NH_3 (*trans*) and ≡N–C distances are calculated to be shortest for R = $C_6H_4NO_2$-4 and longest for R = Bu^t. While there is excellent agreement with the experimental C–N(imide) bond lengths, the experimental Ti–N (*trans*) distance is shortest for R = C_6H_5 but for the calculated structures it is shortest for R = $C_6H_4NO_2$-4. Closer examination shows that the calculations overestimate the Ti–N (*trans*) bond length for R = Bu^t and C_6H_5 by 0.007 and 0.022 Å respectively (see above), but *underestimate* that for R = $C_6H_4NO_2$-4 by 0.014 Å. Given that all of the Ti–N (*cis*) distances are overestimated by the calculations (by 0.006, 0.027 and 0.025 Å respectively for R = Bu^t, C_6H_5 and $C_6H_4NO_2$-4), the underestimate in the $[Ti(NC_6H_4NO_2\text{-}4)Cl_2(NH_3)_3]$ Ti–N (*trans*) distance is the principal reason that the resultant calculated *trans* influence for this molecule is 0.039 Å less than experiment, by contrast with the much smaller discrepancies for R = Bu^t and C_6H_5 (average differences being 0.001 and 0.005 Å, respectively). The calculations therefore suggest that variation of the imido R group not only produces significantly different structural influences, but also different *trans* influences. The latter result could not be confidently concluded from the experimental data because the difference in *trans* influences were not significant compared to the errors in these differences (see Table 1).

‡ In our calculations we have replaced the pyridine ligands of the real compounds by NH_3 groups for reasons of computational feasibility. The model compounds have 21 fewer atoms than their pyridine analogues, which makes an enormous difference to the computing time required (already very large, given the lack of symmetry). In principle, pyridine has the ability to function as both a σ and a π ligand, (ammonia can only be a σ donor). However, if there is a π interaction in metal–pyridine complexes the pyridine will function as a π acceptor, not as a π donor.[26] Hence in d^0 systems such as our model complexes it can only be a σ donor, and thus the replacement of pyridine by NH_3 is justified. In doing so we are not without precedent. See, for example, ref. 27, in which the 'presumably innocent' pyridine ligand is modelled by H^-. We also note that the excellent agreement between the calculated geometries of the model compounds and the experimentally determined geometries of the pyridine systems is good evidence that NH_3 is a sensible replacement for pyridine.

§ Throughout this work the imido–Ti linkages are drawn 'N≡Ti' to represent the formal N–Ti valence bond order of three (*i.e.* a pseudo $\sigma^2\pi^4$ triple bond). For ease of representation we have omitted the formal charges that this description requires.

Table 1 Comparison of selected X-ray crystallographic bond lengths and angles for the complexes $[Ti(NR)Cl_2(py)_3]$ (R = Bu^t, C_6H_5 or $C_6H_4NO_2$-4) with the calculated values of the title complexes in which the py groups are replaced with ammonia ligands[a]

		R = Bu^t	R = C_6H_5	R = $C_6H_4NO_2$-4
Ti≡N/Å	Exp.	1.705(3) 1.706(3)	1.714(2)	1.722(3)
	Calc.	1.711	1.730	1.739
Ti–N (*cis*)/Å	Exp.	2.247(3), 2.249(3) 2.255(3), 2.258(3)	2.225(2), 2.229(3)	2.228(2)
	Calc.	2.259, 2.256 (av = 2.258)	2.253, 2.254 (av = 2.254)	2.254, 2.251 (av = 2.253)
Ti–N (*trans*)/Å	Exp.	2.450(3) 2.440(3)	2.410(3)	2.428(3)
	Calc.	2.452	2.432	2.414
trans Influence/Å	Exp.	0.203(4), 0.201(4) 0.185(4), 0.182(4)	0.181(4), 0.185(4)	0.200(4)
	Calc.	0.194	0.178	0.161
Ti–Cl/Å	Exp.	2.4316(13), 2.4358(13) 2.4313(14), 2.4516(14)	2.4129(10) 2.4157(10)	2.380(1)
	Calc.	2.406, 2.446 (av = 2.426)	2.403, 2.396 (av = 2.400)	2.386, 2.387 (av = 2.387)
≡N–C/Å	Exp.	1.455(5) 1.446(5) (av = 1.451)	1.382(4)	1.359(4)
	Calc.	1.444	1.371	1.359
N≡Ti–N (*cis*)/°	Exp.	95.32(12), 97.55(13) 94.39(13), 99.18(13)	94.40(10), 92.68(10)	97.66(2)
	Calc.	92.94, 92.71 (av = 92.83)	90.88, 91.22 (av = 91.05)	90.16, 90.51 (av = 90.34)
N≡Ti–N (*trans*)/°	Exp.	176.23(14) 175.96(13)	176.26(10)	180
	Calc.	179.79	179.70	179.62
N≡Ti–Cl/°	Exp.	100.85(12), 94.84(12) 95.32(12), 98.32(12)	96.38(9), 97.57(9)	95.33(5)
	Calc.	100.76, 101.57 (av = 101.17)	101.24, 100.85 (av = 101.05)	100.88, 100.50 (av = 100.69)
C–N≡Ti/°	Exp.	174.8(3) 171.7(3)	177.5(2)	180
	Calc.	177.27	179.88	179.12

[a] Experimental data from ref. 8. For $[Ti(NBu^t)Cl_2(py)_3]$ the two sets of figures (one below the other) correspond to the two crystallographically independent molecules; for $[Ti(NC_6H_4NO_2\text{-}4)Cl_2(py)_3]$ the molecules lie on a crystallographic twofold axis passing through the C–N≡Ti–N (*trans*) vector and so there is only one value of Ti–Cl, Ti–N *etc.* and N≡Ti–N (*trans*) must be 180°.

We have performed a series of calculations on $[Ti(NC_6H_4NO_2\text{-}4)Cl_2(NH_3)_3]$ in which all of the bond lengths and angles were set to their optimised values except the Ti–NH_3 (*trans*) distance, which was varied from 2.36 to 2.45 Å in steps of 0.01 Å. The total energy of the molecule varied by only 0.6 kJ mol^{-1} from the least stable (Ti–NH_3 (*trans*) = 2.36 Å) to the most stable geometry (Ti–NH_3 (*trans*) = 2.41 Å), indicating that the potential curve for elongation of the Ti–NH_3 (*trans*) distance at the otherwise optimised geometry is virtually flat. The computationally determined trend toward decreasing *trans* influence in the order $[Ti(NBu^t)Cl_2(NH_3)_3] > [Ti(NC_6H_5)Cl_2(NH_3)_3] > [Ti(NC_6H_4NO_2\text{-}4)Cl_2(NH_3)_3]$ must be viewed in the light of this flat Ti–NH_3 (*trans*) potential curve, *i.e.* it should be recognised that the energy differences between geometries with different *trans* influences are very small. Nevertheless, the $Bu^t > C_6H_5 > C_6H_4NO_2$-4 trend in calculated *trans* influence is a recurring theme of the calculations reported in this paper (as well as many other calculations on these molecules conducted with different computational parameters[28]) and we therefore feel confident in suggesting that isolated molecules of $[Ti(NBu^t)Cl_2(NH_3)_3]$, $[Ti(NC_6H_5)Cl_2(NH_3)_3]$ and $[Ti(NC_6H_4NO_2\text{-}4)Cl_2(NH_3)_3]$ (and their pyridine analogues) would display this trend in *trans* influence.

The calculations, of course, treat each molecule in isolation, while the X-ray crystallographic data are obtained from molecules which are subject to the intermolecular effects of crystal packing forces. These forces are entirely capable of altering the Ti–py (*trans*) distance from that which it might prefer to adopt in an isolated $[Ti(NC_6H_4NO_2\text{-}4)Cl_2(py)_3]$ molecule to that observed in the solid state, as our calculations reveal that there is a negligible energy change over a 0.10 Å range of Ti–N (*trans*) distances. This view is supported by the crystallographic data for $[Ti(NBu^t)Cl_2(py)_3]$ which show that the experimental *trans* influence varies by *ca*. 0.02 Å from 0.182(4) to 0.203(4) for the two crystallographically independent molecules. Our conclusion, therefore, is that the experimental observation of different structural but similar *trans* influences in $[Ti(NR)Cl_2(py)_3]$ (R = Bu^t, C_6H_5 or $C_6H_4NO_2$-4) is most likely to have an inter- rather than an intra-molecular origin.

The origin of the *trans* influence in $[Ti(NR)Cl_2(NH_3)_3]$ (R = Bu^t, C_6H_5 or $C_6H_4NO_2$-4)

(i) The effects of varying the RN≡Ti–Cl angle. Both theory and experiment clearly indicate that there is a marked difference between the Ti–N (*cis*) and Ti–N (*trans*) distances in $[Ti(NR)Cl_2(NH_3)_3]$ (R = Bu^t, C_6H_5 or $C_6H_4NO_2$-4) and their pyridine analogues, and it is important that we establish the cause of this difference. In a 1995 contribution, Lyne and Mingos probed the electronic and geometric structures of pseudo-octahedral $[OsNCl_5]^{2-}$ using density functional theory.[6] They initially optimised the geometry within C_{4v} symmetry and confirmed that theory satisfactorily reproduced the experimental structure. Subsequently they set the N≡Os–Cl (*cis*) bond angles to 90° and analysed the variations in the energies of the individual molecular orbitals (MOs) as well as the overall electronic and steric interaction energies as the N≡Os–Cl (*cis*) bond angles were allowed to relax to their value in the optimised structure (96°). Their principal conclusions can be summarised as follows. The second highest occupied MO (the 4e orbital) is π bonding between the N atom and the Os but π antibonding between the metal and the *cis* Cl. This MO is stabilised as the Cl

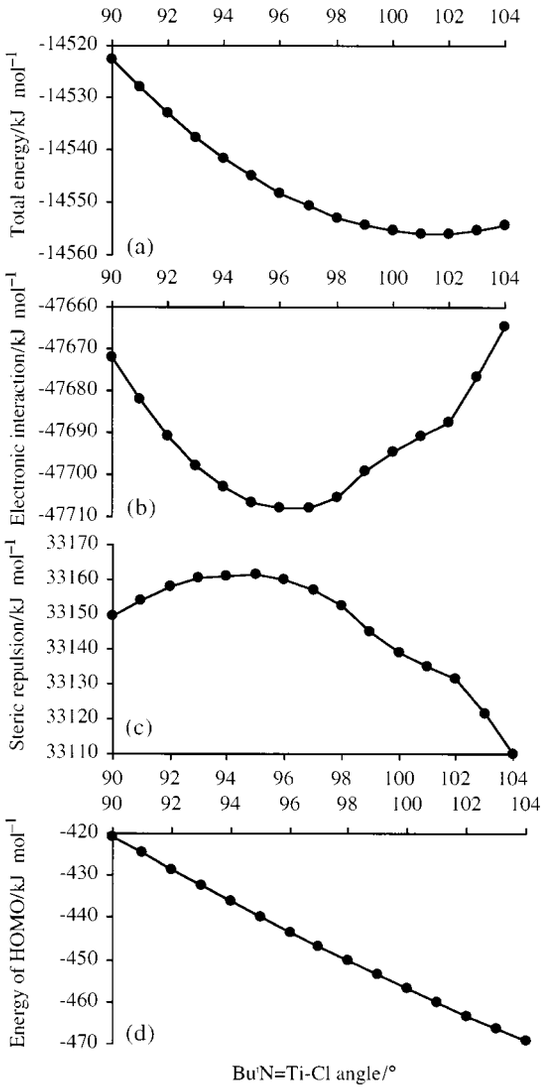

Fig. 1 Plots of (a) total molecular bonding energy (b) electronic interaction energy (c) steric repulsion energy and (d) energy of highest occupied molecular orbital (all kJ mol^{-1}) against $Bu^tN{\equiv}Ti$–Cl angle (°) for constrained geometry optimisations of $[Ti(NBu^t)Cl_2(NH_3)_3]$.

atoms are moved away from the N (the unfavourable Os–Cl interaction is reduced and the Os≡N bonding interaction is enhanced), and this orbital stabilisation is the driving force for the N≡Os–Cl (*cis*) angle to exceed 90°. As the *cis* Cl atoms move away from the N, non-bonded repulsions with the *trans* Cl cause a lengthening of the Os–Cl (*trans*) bond, thus giving rise to the observed *trans* influence.

So as to make comparison with this previous work, we have undertaken a similar study of $[Ti(NR)Cl_2(NH_3)_3]$ (R = Bu^t, C_6H_5 or $C_6H_4NO_2$-4) in which three series of constrained geometry optimisations (one series for each molecule) have been performed. In these calculations the RN≡Ti–Cl angle was varied from 90° to 104° in steps of 1° and the rest of the geometric parameters were optimised at each RN≡Ti–Cl angle.

Fig. 1 shows the result of this study for $[Ti(NBu^t)Cl_2(NH_3)_3]$. The total molecular bonding energy (a) is broken down into its electronic (b) and steric (c) components (see the section entitled 'Computational and theoretical details' for the definition of these terms), and the energy of the highest occupied molecular orbital (HOMO) is plotted in Fig. 1(d). The equivalent graphs for the other two molecules (not shown) are similar, and the arguments set out below for $[Ti(NBu^t)Cl_2(NH_3)_3]$ are equally applicable to $[Ti(NC_6H_5)Cl_2(NH_3)_3]$ and $[Ti(NC_6H_4NO_2\text{-}4)Cl_2(NH_3)_3]$.

Moving the Cl atoms away from the NBu^t group is initially

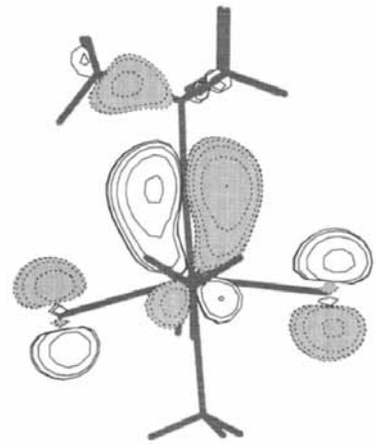

Fig. 2 The 40a highest occupied molecular orbital of $[Ti(NBu^t)Cl_2(NH_3)_3]$, viewed down one of the Ti–NH_3 (*cis*) bonds.

energetically favourable. As the $Bu^tN{\equiv}Ti$–Cl angle increases, however, the total molecular bonding energy levels out, with the most stable geometry (33.33 kJ mol^{-1} more stable than the 90° structure) having a $Bu^tN{\equiv}Ti$–Cl angle of 102° (the values for the $Bu^tN{\equiv}Ti$–Cl angles in the fully optimised structure are 100.76° and 101.57°; Table 1). The electronic interaction is also initially favoured by increasing the $Bu^tN{\equiv}Ti$–Cl angle, becoming most negative at 97° before rising once again. The steric repulsion curve has the opposite profile, maximising at 95° before falling away with increasing $Bu^tN{\equiv}Ti$–Cl angle. The alterations in the electronic interaction are the result of the energy changes of all of the occupied MOs, many of which are very small. It is noticeable, however, that the energy change of the HOMO [Fig. 1(d)] is much greater than that of any of the other orbitals. As can be seen in Fig. 2, this orbital is π bonding between the Ti and the imido N but π antibonding between the Ti and the Cl atoms. Its stabilisation with increasing $Bu^tN{\equiv}Ti$–Cl angle is partly due to the alleviation of the metal–Cl (*cis*) π antibonding interaction, analogous to the 4e MO of $[OsNCl_5]^{2-}$ (there is also a d/p hybridisation at the Ti atom which is enhanced by increasing $Bu^tN{\equiv}Ti$–Cl angle and which favours π overlap between the metal and the imido N[29]). As the $Bu^tN{\equiv}Ti$–Cl angle increases beyond 97° the combined effect of all of the other occupied orbitals overcomes the stabilisation due to the HOMO, but we may conclude that the initial driving force for the $Bu^tN{\equiv}Ti$–Cl angle to exceed 90° is the same in $[Ti(NBu^t)Cl_2(NH_3)_3]$ and $[OsNCl_5]^{2-}$.

The variations in the Cl–N^{im} and Cl–N (NH_3 *trans*) distances as the $Bu^tN{\equiv}Ti$–Cl angle increases give rise to changes in steric interactions which play a major role in shaping Fig. 1(c). We have examined the changes in steric interaction between the Cl atoms and the imido and *trans* NH_3 N atoms by conducting a series of single point calculations in which these atoms were placed at their positions at each step of the $Bu^tN{\equiv}Ti$–Cl angle distortion, and all of the other atoms were removed from the calculation. The steric repulsion between the Cl atoms and the imido N is found to decrease by *ca.* 23 kJ mol^{-1} between $Bu^tN{\equiv}Ti$–Cl = 90° and 102°. By contrast, that between the Cl and the *trans* NH_3 N increases by *ca.* 13 kJ mol^{-1} over the same change of angle. The combination of these two effects accounts for much of the overall change in steric repulsion between $Bu^tN{\equiv}Ti$–Cl = 90° and 102°.¶

We have repeated the Cl–N (NH_3 *trans*) interaction calculations with the *trans* NH_3 N fixed at its position in the $Bu^tN{\equiv}Ti$–Cl = 90° structure, in order to compare the steric inter-

¶ The cause of the initial increase in overall steric repulsion is not clear. It does not arise from the Cl–N^{im}/N (NH_3 *trans*) interactions as the former decreases over the $Bu^tN{\equiv}Ti$–Cl angle range 90–95° and the latter is almost constant.

Table 2 Calculated Ti–NH_3 (*trans*) and Ti–NH_3 (*cis*) distances (Å) for $[Ti(NR)Cl_2(NH_3)_3]$ (R = Bu^t, C_6H_5 or $C_6H_4NO_2$-4) at RN≡Ti–Cl = 90° and in the fully optimised structure (see Table 1)

	R = Bu^t		R = C_6H_5		R = $C_6H_4NO_2$-4	
	RN≡Ti–Cl = 90°	Fully optimised structure	RN≡Ti–Cl = 90°	Full optimised structure	RN≡Ti–Cl = 90°	Fully optimised structure
Ti–NH_3 (*cis*)	2.258	2.258	2.253	2.254	2.251	2.253
Ti–NH_3 (*trans*)	2.407	2.452	2.390	2.432	2.377	2.414
trans Influence	0.149	0.194	0.137	0.178	0.126	0.161
trans Influence at RN–Ti–Cl = 90° as a percentage of that at the fully optimised geometry	76.8		77.0		78.3	

actions between Cl and *trans* NH_3 N at Ti–NH_3 (*trans*) = 2.407 Å with that at Ti–NH_3 (*trans*) = 2.452 Å. The difference in steric repulsion between the Cl atoms and the *trans* NH_3 N at the two Ti–NH_3 (*trans*) distances (with the Bu^tN≡Ti–Cl angle = 102°) is only 2 kJ mol^{-1}, the longer Ti–NH_3 (*trans*) distance resulting in the smaller steric interaction. We may therefore conclude that the reduction in steric repulsion between the Cl atoms and the *trans* NH_3 N atom is indeed a driving force for lengthening of the Ti–NH_3 (*trans*) bond, but that the effect is not large.

In their analysis of $[OsNCl_5]^{2-}$, Lyne and Mingos[6] compared the electronic interaction and steric repulsion energies at N≡Os–Cl (*cis*) angles of 90° and 96° (the optimised value). They found that increasing the angle led to an increase in the electronic interaction energy (*i.e.* it became more negative) and a decrease in the steric repulsion, *i.e.* that the overall molecular stabilisation at the optimised geometry is a combination of favourable electronic and steric factors. This was also their conclusion from similar studies on the square based pyramidal $[OsNCl_4]^-$. The data in Fig. 1 are more complete than those of Lyne and Mingos in that many more geometries are considered, but the conclusion is similar. At the most stable geometry (Bu^tN≡Ti–Cl = 102°) the electronic interaction energy is greater than at Bu^tN≡Ti–Cl = 90° and the steric repulsion is less.

Thus the overall molecular stability is increased by moving the Cl atoms away from the imido ligand. We now examine in more detail the effect of this process on the *trans* influence. Table 2 presents the calculated Ti–NH_3 (*trans*) and Ti–NH_3 (*cis*) distances for all three of the title molecules at their fully optimised geometries and at the partially optimised geometries with the RN≡Ti–Cl angles fixed at 90°.‖ It may be seen that constraining the RN≡Ti–Cl angle has a negligible effect on the Ti–NH_3 (*cis*) distances. Indeed, the Ti–NH_3 (*cis*) bond lengths are very similar in all three molecules. By contrast, the value of the Ti–NH_3 (*trans*) distance is significantly altered by constraining the RN≡Ti–Cl angle to 90°, with a reduction from the fully optimised bond length and thus a reduction in the *trans* influence. However, even with the RN≡Ti–Cl angle set to 90° there remains a large *trans* influence, and it would therefore appear that the moving of the Cl atoms away from the imido ligand accounts for only *ca*. 25% of the *trans* influence in the title molecules.**

Lyne and Mingos[6] do not detail the effect of increasing the N≡Os–Cl (*cis*) angle on the *trans* influence in $[OsNCl_5]^{2-}$. We have therefore conducted a series of constrained geometry optimisations on this complex, in C_{4v} symmetry, in which the N≡Os–Cl (*cis*) angle was altered from 90° to 96° in steps of 1°. Our calculations do not reproduce exactly the results of Lyne and Mingos, presumably due to the different parameters (basis sets, functionals and relativistic corrections) employed.†† Our optimised N≡Os–Cl (*cis*) angle is 93.96°, 2° less than that reported previously, and the calculated *trans* influence at this angle (0.129 Å) is somewhat less than the 0.2 Å at N≡Os–Cl (*cis*) = 96° obtained by Lyne and Mingos. The most significant result of the present $[OsNCl_5]^{2-}$ calculations is that at an N≡Os–Cl (*cis*) angle of 90° the *trans* influence is only 0.049Å, in contrast to the 0.129 Å found at 94° (and the 0.194 Å obtained at 96°). Thus the effects of the increase in the N≡Os–Cl (*cis*) angle account for the majority of the *trans* influence in $[OsNCl_5]^{2-}$, quite different from the situation in $[Ti(NR)Cl_2(NH_3)_3]$ (R = Bu^t, C_6H_5 or $C_6H_4NO_2$-4).

(ii) Analysis of the Ti–NH_3 bonding. So what is the cause of the *ca*. 75% of the *trans* influence that is not due to the moving of the Cl atoms away from the imido groups? We can make progress in answering this question by consideration of the MO structure of the title compounds at the constrained geometries discussed above, *i.e.* in which the RN≡Ti–Cl angles are set to 90° and the remaining parameters allowed to optimise. This should ensure that any residual non-bonded repulsions between the Cl atoms and the *trans* NH_3 ligand are minimised and similar between the three molecules. Fig. 3 presents an MO energy level diagram for the 17 highest occupied orbitals of $[Ti(NBu^t)Cl_2(NH_3)_3]$ at the partially optimised geometry (RN≡Ti–Cl angle = 90°). The principal bonding characteristics of each MO are also given. The absence of symmetry elements means that all of the MOs carry the same Mulliken symbol, 'a', and that all of the atomic orbital (AO) basis functions (more than 300) can in principle contribute to any MO. In practice, however, the principal bonding characteristics of the MOs are readily identified.

Aside from the 40a HOMO, three other orbitals are labelled on Fig. 3. These are the 24a, 27a and 32a levels, which are also indicated by dashed lines. These MOs are important as they are the only ones which involve discernable interaction between the Ti and the NH_3 groups. Fig. 4 presents plots of these levels, from which it may be seen that the 27a MO (Fig. 4(b)) is bonding between the metal and all the NH_3 groups. The 24a MO (Fig. 4(a)) is an in-phase combination of both *cis* and *trans* NH_3 functions which is also bonding between the Ti and the *cis* NH_3, but the direct Ti–NH_3 (*trans*) interaction (*i.e.* along the Ti–N vector) is antibonding. Furthermore, the 32a MO (Fig. 4(c)), which has no contribution from the *cis* NH_3 groups, is

‖ The N≡Ti–N (*cis*) angles and Ti≡N distances obtained in the partially constrained geometries are as follows: $[Ti(NBu^t)Cl_2(NH_3)_3]$ 93.18°, 93.50°, 1.706 Å; $[Ti(NC_6H_5)Cl_2(NH_3)_3]$ 92.13°, 91.58°, 1.725 Å; $[Ti(NC_6H_4NO_2\text{-}4)Cl_2(NH_3)_3]$ 92.38°, 91.85°, 1.734 Å.

** Note that the reduction in *trans* influence is, in percentage terms, almost exactly the same for all three molecules and hence the trend to increasing *trans* influence in the order $C_6H_4NO_2$-4 < C_6H_5 < Bu^t is the same at both the optimised N≡Ti–Cl angle and at N≡Ti–Cl = 90°.

†† Note that the calculated parameters (*i.e.* ADF Type IV basis sets and the combination of the Vosko, Wilk and Nusair local density parameterisation and the gradient corrections of Becke and Perdew) used by us for $[OsNCl_5]^{2-}$ are the same as those used for the Ti molecules (with the exception of relativistic frozen cores), in order to facilitate comparison between the two sets of results.

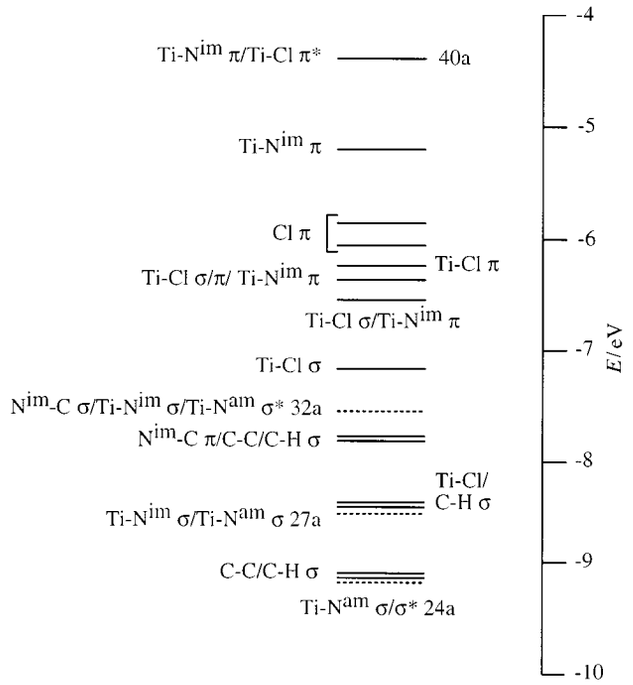

Fig. 3 Molecular orbital energy level diagram for the 17 highest occupied molecular orbitals of $[Ti(NBu^t)Cl_2(NH_3)_3]$ at a partially optimised geometry in which the $Bu^tN{\equiv}Ti{-}Cl$ angle is fixed at 90°.

also antibonding between the Ti and the *trans* NH_3. Thus while there is no filled antibonding MO to counter the Ti–NH_3 (*cis*) bonding of the 24a and 27a levels, the Ti–NH_3 (*trans*) bonding in the 27a orbital is opposed by the Ti–NH_3 (*trans*) antibonding properties of the 24a and 32a MOs. The reduced Ti–NH_3 (*trans*) bonding compared to the Ti–NH_3 (*cis*) manifests itself as a relative lengthening of the Ti–NH_3 (*trans*) bond, *i.e.* as a *trans* influence.

Before moving on to discuss the compositions of the 24a, 27a and 32a MOs in more detail, it is worth comparing the calculated Ti–NH_3 interactions with those expected on group theoretical grounds. Taking a localised view of the Ti–NH_3 interactions, we would anticipate three Ti–NH_3 bonding MOs. In the pseudo C_{2v} symmetry of the title compounds, these three MOs would transform as $2 \times a_1$ and $1 \times b_1$, the former involving both *cis* and *trans* Ti–NH_3 bonding and the latter being confined to Ti–NH_3 (*cis*) bonding. Fig. 4 suggests that the 24a and 27a MOs may be identified with the pseudo a_1 symmetry C_{2v} levels, although it is noticeable that the 24a orbital does not have the anticipated Ti–NH_3 (*trans*) bonding character. Interestingly, none of the MOs in Fig. 4 has pseudo b_1 character. In fact, MOs 28a and 29a (Fig. 3) are of pseudo b_1 symmetry in that they have significant out of phase contributions from the *cis* NH_3 N atoms (as well as large Bu^t content) and no *trans* NH_3 character, but neither of these MOs has any Ti content.

It would therefore appear that the pseudo C_{2v} approach is not completely supported by the C_1 calculations. This may well arise from the Ti–NH_3 bonding being distributed (and therefore 'diluted') over many more MOs in the C_1 calculations than the three expected from a pseudo C_{2v} analysis. It may also be a consequence of the reduction in symmetry resulting in a mixing of orbital character, or indeed be due to failings in the localised approach to Ti–NH_3 bonding. It is clear, however, that the only MOs with a Ti–NH_3 interaction large enough to be visible in orbital representations of the kind shown in Fig. 4 (and 2 and 5) are the 24a, 27a and 32a levels.

The contributions of the Ti, imido N and *cis* and *trans* ammonia N AOs to these MOs are given in Table 3. The primarily Ti–NH_3 (*cis*) bonding in the 24a level is confirmed by the observation that the only Ti d AO contribution to this MO is d_{z^2} (the axis system imposed by ADF orients the Ti–NH_3 (*cis*)

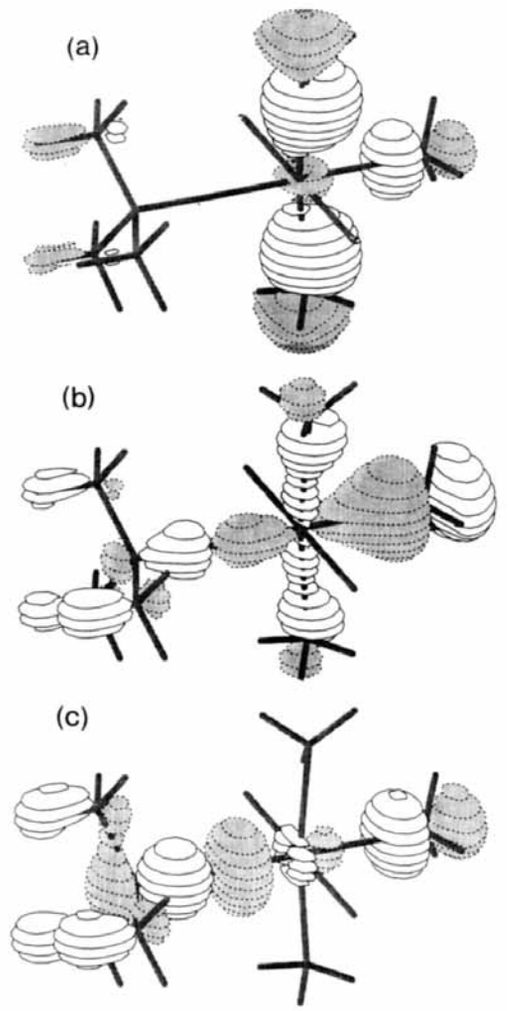

Fig. 4 The (a) 24a, (b) 27a and (c) 32a molecular orbitals of $[Ti(NBu^t)Cl_2(NH_3)_3]$.

bonds approximately along the *z* axis, with the *x* axis being the C–N≡Ti–NH_3 (*trans*) vector) and by the large contribution from the *cis* ammonia N atoms. The 27a has both d_{z^2} and $d_{x^2-y^2}$ character in keeping with its bonding between the Ti and all three NH_3 groups. The 32a has no Ti contribution in the *z* direction, as is clear from Fig. 4(c).‡‡

The compositions of the only MOs of $[Ti(NR)Cl_2(NH_3)_3]$ (R = C_6H_5 or $C_6H_4NO_2$-4) that contain any contribution from both the Ti and the N atoms of the NH_3 groups are also given in Table 3. Turning first to $[Ti(NC_6H_4NO_2\text{-}4)Cl_2(NH_3)_3]$, the 32a MO is similar to its $[Ti(NBu^t)Cl_2(NH_3)_3]$ analogue (24a). The Ti contribution to the 34a level is also similar to that in the 27a of $[Ti(NBu^t)Cl_2(NH_3)_3]$, but the *trans* ammonia N character is much reduced. This suggests that the 34a MO of $[Ti(NC_6H_4NO_2\text{-}4)Cl_2(NH_3)_3]$ is less Ti–NH_3 (*trans*) bonding than the 27a of $[Ti(NBu^t)Cl_2(NH_3)_3]$, and this is supported by the plot of this orbital shown in Fig. 5(a). Interestingly, the Ti contribution to the 36a of $[Ti(NC_6H_4NO_2\text{-}4)Cl_2(NH_3)_3]$ is

‡‡ It is noticeable that the Ti contributions to all three MOs are quite small, rather smaller, in fact, than would appear to be the case from Fig. 4. It is difficult to know if this is merely a reflection of the vagaries of the Mulliken population analysis method, or genuinely reflects the Ti contribution. Given that the Ti is formally d^0 we would not expect any of the occupied MOs to be predominantly Ti-based. Indeed, with the exception of the HOMO and second HOMO, which are Ti≡N π bonding in each molecule and have Ti contributions of *ca.* 20–30%, none of the valence MOs has greater than *ca.* 15% Ti character. Thus whether the Ti contributions given in Table 3 are really so small is open to question. The bonding characteristics of each MO (as evidenced by Fig. 4) are, however, quite clear.

Table 3 Percent contributions of the Ti, imido N and *trans* and *cis* ammonia N atoms (Mulliken population analysis) to the MOs of $[Ti(NR)Cl_2(NH_3)_3]$ (R = Bu^t, C_6H_5 or $C_6H_4NO_2$-4) with both Ti and ammonia N character, at the partially optimised geometries with RN≡Ti–Cl constrained to 90°[a]

		Composition			
Molecule	Orbital	% Ti	% imido N	% *trans* ammonia N	% *cis* ammonia N[b]
$[Ti(NBu^t)Cl_2(NH_3)_3]$	24a	4.5 d_{z^2} 4.4 s	–	12.1 p_x	25.4 p_z 1.9 s 0.9 p_x
	27a	8.0 d_{z^2} 4.2 $d_{x^2-y^2}$	4.0 p_x	37.2 p_x 4.0 s	6.2 p_z
	32a	2.9 $d_{x^2-y^2}$ 1.0 p_x	26.8 p_x	19.4 p_x 2.3 s	–
$[Ti(NC_6H_5)Cl_2(NH_3)_3]$	26a	4.7 $d_{x^2-y^2}$ 2.8 s	16.1 p_x	11.8 p_x	3.9 p_z
	29a	1.0 d_{z^2} 3.2 p_z 0.4 $d_{x^2-y^2}$	–	15.4 p_x 1.7 s	21.3 p_z 2.1 s 0.8 p_x 0.9 p_y
	30a	1.9 d_{z^2} 1.9 p_z 0.6 $d_{x^2-y^2}$	–	24.1 p_x 2.6 s	14.4 p_z 1.2 s 0.6 p_x
	31a	1.0 $d_{x^2-y^2}$	16.2 p_x	16.6 p_x 1.1 s	–
$[Ti(NC_6H_4NO_2\text{-}4)Cl_2(NH_3)_3]$	32a	2.6 d_{z^2} 0.5 $d_{x^2-y^2}$ 1.1 p_x 3.7 s	1.8 p_x	13.6 p_x	20.4 p_z 1.6 s 0.7 p_x 0.6 p_y
	34a	9.3 d_{z^2} 5.1 $d_{x^2-y^2}$	13.0 p_x	6.3 p_x 0.7 s	9.8 p_z 0.9 s 0.4 p_x
	36a	0.9 d_{z^2} 0.1 $d_{x^2-y^2}$ 0.1 s	14.2 p_x	47.7 p_x 5.3 s	–

[a] Note that the C–N≡Ti–NH_3 vector is the *x* axis and the Ti–NH_3 (*cis*) bonds lie approximately along the *z* axis. [b] Contributions *per atom*, *i.e.* as an average of the two *cis* ammonia N atom contributions.

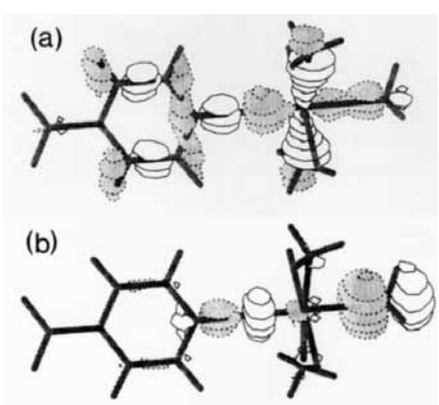

Fig. 5 The (a) 34a and (b) 36a molecular orbitals of $[Ti(NC_6H_4NO_2\text{-}4)Cl_2(NH_3)_3]$.

smaller than in the 32a of $[Ti(NBu^t)Cl_2(NH_3)_3]$, and is not oriented along the *x* axis. Thus, notwithstanding the large *trans* ammonia N contribution to this orbital, it is less Ti–NH_3 (*trans*) antibonding than the 32a MO of $[Ti(NBu^t)Cl_2(NH_3)_3]$. This can be seen in Fig. 5(b). Hence the interaction of the Ti with the *trans* NH_3 group in $[Ti(NC_6H_4NO_2\text{-}4)Cl_2(NH_3)_3]$ features both reduced bonding and antibonding in comparison with $[Ti(NBu^t)Cl_2(NH_3)_3]$. Given that the calculated *trans* influence for RN≡Ti–Cl = 90° is 0.023 Å less in the $C_6H_4NO_2$-4 molecule, the conclusion must be that the reduced antibonding of the 36a MO is more significant than the reduced bonding of the 34a.

Table 2 indicates that there is very little difference between the Ti–NH_3 (*cis*) distances in the partially optimised geometries of $[Ti(NBu^t)Cl_2(NH_3)_3]$ and $[Ti(NC_6H_4NO_2\text{-}4)Cl_2(NH_3)_3]$. This is supported by the data in Table 3, which show that the average *cis* ammonia N atom p_z contribution to the Ti–NH_3 (*cis*) bonding MOs is almost exactly the same in the Bu^t and $C_6H_4NO_2$-4 molecules (15.8% p_z per *cis* ammonia N atom in 24a and 27a of $[Ti(NBu^t)Cl_2(NH_3)_3]$; 15.1% p_z per *cis* ammonia N atom in 32a and 34a of $[Ti(NC_6H_4NO_2\text{-}4)Cl_2(NH_3)_3]$).

$[Ti(NC_6H_5)Cl_2(NH_3)_3]$ is different from $[Ti(NR)Cl_2(NH_3)_3]$ (R = Bu^t or $C_6H_4NO_2$-4) in that four MOs have a contribution from both the Ti atom and the N atoms of the ammonia groups. The 26a level is similar to the 27a MO of $[Ti(NBu^t)Cl_2(NH_3)_3]$ in its nature and extent of Ti–NH_3 (*trans*) bonding, although it has reduced Ti–NH_3 (*cis*) bonding. The 29a and 30a levels are similar to the 24a MO of $[Ti(NBu^t)Cl_2(NH_3)_3]$, except that each of the two orbitals bonds primarily with just one of the *cis* NH_3 groups. The Ti–NH_3 (*cis*) bonding of the 24a MO of $[Ti(NBu^t)Cl_2(NH_3)_3]$ is therefore spread over two orbitals in $[Ti(NC_6H_5)Cl_2(NH_3)_3]$, both of which feature the small Ti–NH_3 (*trans*) antibonding interaction of the 24a level of $[Ti(NBu^t)Cl_2(NH_3)_3]$. The 31a orbital is very similar to the 32a MO of $[Ti(NBu^t)Cl_2(NH_3)_3]$, *i.e.* it is Ti–NH_3 (*trans*) antibonding, albeit with reduced metal and *trans* ammonia N contributions.

The calculated *trans* influence of $[Ti(NC_6H_5)Cl_2(NH_3)_3]$ at a C_6H_5N≡Ti–Cl angle of 90° is midway between that of $[Ti(NBu^t)Cl_2(NH_3)_3]$ and $[Ti(NC_6H_4NO_2\text{-}4)Cl_2(NH_3)_3]$ (Table 2). While it is unlikely that this difference (or indeed any geometric trend) can be attributed solely to variations in the composition of any one MO, it is worth noting that the antibonding character of the 31a MO of $[Ti(NC_6H_5)Cl_2(NH_3)_3]$ is midway between the corresponding MOs of $[Ti(NBu^t)Cl_2(NH_3)_3]$ and $[Ti(NC_6H_4NO_2\text{-}4)Cl_2(NH_3)_3]$.

(iii) The effects of varying the Ti≡N distance. We have already demonstrated that variation of the imido R group produces significantly different *trans* influences in the title compounds. It is important to establish if these differences arise solely from

Table 4 Calculated Ti–NH_3 (*trans*) and Ti–NH_3 (*cis*) distances (Å) for $[Ti(NR)Cl_2(NH_3)_3]$ (R = Bu^t, C_6H_5 or $C_6H_4NO_2$-4) at RN≡Ti–Cl = 90° and three different values of Ti≡N

Molecule	Ti≡N	Ti–NH_3 (*trans*)	Ti–NH_3 (*cis*)	*trans* Influence
$[Ti(NBu^t)Cl_2(NH_3)_3]$	1.711	2.407	2.258	0.149
	1.730	2.397	2.256	0.141
	1.739	2.396	2.257	0.139
$[Ti(NC_6H_5)Cl_2(NH_3)_3]$	1.711	2.396	2.254	0.142
	1.730	2.390	2.253	0.137
	1.739	2.386	2.251	0.135
$[Ti(NC_6H_4NO_2\text{-}4)Cl_2(NH_3)_3]$	1.711	2.382	2.252	0.130
	1.730	2.377	2.252	0.125
	1.739	2.377	2.251	0.126

the different Ti–N distances within the three molecules or if, for a given Ti≡N distance, alteration of the R group generates a different *trans* influence. In other words, does the nature of the imido R group have a primary effect on the *trans* influence, or a secondary one in that altering R changes the Ti≡N distance and thus the *trans* influence?

In order to address this question we have conducted three series of constrained geometry optimisations (one series of each molecule) in which the RN≡Ti–Cl angle was set at 90° and the Ti≡N distance fixed at its value in the fully optimised structures of the other two molecules, *e.g.* for $[Ti(NBu^t)Cl_2(NH_3)_3]$ Ti≡N was set to 1.730 and 1.739 Å, these being the values for $[Ti(NC_6H_5)Cl_2(NH_3)_3]$ and $[Ti(NC_6H_4NO_2\text{-}4)Cl_2(NH_3)_3]$ respectively. The results of these calculations are given in Table 4 (which also includes the data for the previous constrained geometry optimisations from Table 2).

It is clear that *both* the Ti≡N distance *and* the nature of the R group affect the *trans* influence. Thus, for a given Ti≡N distance, the *trans* influence increases in the order $C_6H_4NO_2$-4 < C_6H_5 <Bu^t. In addition, for a given R group the *trans* influence generally increases with decreasing Ti≡N distance. There is an almost linear relationship between the *trans* influence and Ti≡N distance for R = C_6H_5 and Bu^t, while the trend in $[Ti(NC_6H_4NO_2\text{-}4)Cl_2(NH_3)_3]$ is broken by the *trans* influence at Ti≡N = 1.739 Å, which is greater than that at Ti≡N = 1.730 Å (albeit by only 0.001 Å!).

Conclusions

In this contribution, modern density functional theory has been used to probe the geometric and electronic structures of $[Ti(NR)Cl_2(NH_3)_3]$ (R = Bu^t, C_6H_5 or $C_6H_4NO_2$-4), models for the corresponding crystallographically characterised pyridine complexes $[Ti(NR)Cl_2(py)_3]$.[7,8] From these calculations, we have reached a number of important conclusions concerning the bonding in these compounds as well as that within $[OsNCl_5]^{2-}$, and these are summarised below.

1 Full geometry optimisations of $[Ti(NR)Cl_2(NH_3)_3]$ (R = Bu^t, C_6H_5 or $C_6H_4NO_2$-4) produce true minimum energy structures which agree extremely well with experimental data for the analogous pyridine systems. Each molecule is calculated to have a significant *trans* influence, and this decreases in the order $[Ti(NBu^t)Cl_2(NH_3)_3]$ > $[Ti(NC_6H_5)Cl_2(NH_3)_3]$ > $[Ti(NC_6H_4NO_2\text{-}4)Cl_2(NH_3)_3]$. The experimental observation of no significantly different *trans* influences in $[Ti(NR)Cl_2(py)_3]$ (R = Bu^t, C_6H_5 or $C_6H_4NO_2$-4) is rationalised computationally by the observation that the potential curve for elongation of the Ti–NH_3 *trans* distance is essentially flat, *i.e.* that intermolecular forces in the solid state are entirely capable of altering the Ti–py *trans* distance from its preferred isolated molecule value to that observed crystallographically.

2 The *trans* influence in the title molecules is found to have two causes. (a) The highest occupied molecular orbital is in each case π bonding between the imido N atom and the Ti, but π antibonding between the metal and the *cis* Cl atoms. Bending the Cl atoms away from the NR group reduces the unfavourable Ti–Cl interaction and strengthens that between the Ti and the imido N. Subsequently, steric repulsions between the Cl atoms and the *trans* NH_3 N atom lead to a lengthening of the Ti–NH_3 *trans* distance. This component of the *trans* influence is therefore a combination of π electronic and steric effects, but accounts for only *ca*. 25% of the total *trans* influence in each case. This is in contrast to previous and present studies of $[OsNCl_5]^{2-}$, which reveal that the π orbital driven *cis–trans*–Cl repulsion is responsible for the majority of the *trans* influence in this complex. (b) The remaining *ca*. 75% of the *trans* influence in the title compounds is found to be purely electronic in origin. Analysis of the electronic structures at partially optimised geometries in which the RN≡Ti–Cl angles are fixed to 90° reveals that there are two filled molecular orbitals which are antibonding between the Ti and the *trans* NH_3 group. In contrast, there are no occupied molecular orbitals which are Ti–NH_3 *cis* antibonding. This 'intrinsic' *trans* influence decreases in the order $[Ti(NBu^t)Cl_2(NH_3)_3]$ > $[Ti(NC_6H_5)Cl_2(NH_3)_3]$ > $[Ti(NC_6H_4NO_2\text{-}4)Cl_2(NH_3)_3]$. This order has been rationalised by examination of the composition of the Ti–NH_3 *cis* and *trans* bonding and antibonding molecular orbitals.

3 Both the nature of the imido R group and the Ti≡N distance are found to affect the *trans* influence. For a given Ti≡N distance, the *trans* influence increases in the order $C_6H_4NO_2$-4 < C_6H_5 < Bu^t, while for a given R group the *trans* influence generally increases with decreasing Ti≡N distance.

In summary, therefore, we may conclude that the *trans* influence in the title molecules arises from a complex interplay of π orbital driven steric effects (*ca*. 25%) and intrinsic electronic factors (*ca*. 75%). Both of these effects are dependent upon the nature of the imido R substituent, with Bu^t producing the largest *trans* influence and $C_6H_4NO_2$-4 the smallest.

Acknowledgements

N. K. thanks the Royal Society for equipment grants, and the UK Computational Chemistry Working Party for a grant of computer time on the EPSRC's 'Columbus/Magellan' facility. P. M. thanks the Royal Society, the EPSRC and the Leverhulme Trust. P. M. is the Royal Society of Chemistry Sir Edward Frankland Fellow for 1998–1999.

References

1 W. A. Nugent and J. M. Mayer, *Metal-ligand multiple bonds*, Wiley-Interscience, New York, 1988.
2 J. K. Burdett and T. A. Albright, *Inorg. Chem.*, 1979, **18**, 2112.
3 E. M Shustorovich, M. A. Porai-Koshits and Y. A. Busalev, *Coord. Chem. Rev.*, 1975, **17**, 1.
4 D. Bright and J. A. Ibers, *Inorg. Chem.*, 1969, **8**, 709.
5 P. D. Lyne and D. M. P. Mingos, *J. Organomet. Chem.*, 1994, **478**, 141.
6 P. D. Lyne and D. M. P. Mingos, *J. Chem. Soc.*, *Dalton Trans.*, 1995, 1635.
7 P. E. Collier, S. C. Dunn, P. Mountford, O. V. Shishkin and D. Swallow, *J. Chem. Soc.*, *Dalton Trans.*, 1995, 3743.
8 A. J. Blake, P. E. Collier, S. C. Dunn, W.-S. Li, P. Mountford and O. V. Shishkin, *J. Chem. Soc.*, *Dalton Trans.*, 1997, 1549.
9 D. E. Wigley, *Prog. Inorg. Chem.*, 1994, **42**, 239.
10 P. Mountford, *Chem. Commun.*, 1997, 2127.
11 A. J. Blake, P. E. Collier, L. H. Gade, M. McPartlin, P. Mountford, M. Schubart and I. J. Scowen, *Chem. Commun.*, 1997, 1555.
12 P. J. Wilson, A. J. Blake, P. Mountford and M. Schröder, *Chem. Commun.*, 1998, 1007.
13 A. J. Blake, S. C. Dunn, J. C. Green, N. M. Jones, A. G. Moody and P. Mountford, *Chem. Commun.*, 1998, 1235.
14 J. M. McInnes and P. Mountford, *Chem. Commun.*, 1998, 1669.
15 G. te Velde and E. J. Baerends, *J. Comp. Phys.*, 1992, **99**, 84.
16 ADF < 2.3 > , Department of Theoretical Chemistry, Vrije Universiteit, Amsterdam, 1997.
17 T. Ziegler, V. Tschinke, E. J. Baerends, J. G. Snijders and W. Ravenek, *J. Phys. Chem.*, 1989, **93**, 3050.

18 S. H. Vosko, L. Wilk and M. Nusair, *Can. J. Phys.*, 1980, **58**, 1200.
19 A. Becke, *Phys. Rev. A*, 1998, **38**, 3098.
20 J. P. Perdew, *Phys. Rev. B*, 1986, **33**, 8822.
21 R. S. Mulliken, *J. Chem. Phys.*, 1955, **23**, 1833.
22 For details of both MOLDEN and ADFrom, the reader is directed to http://www.caos, kun.nl/~schaft/molden/molden.html
23 T. Ziegler and A. Rauk, *Theor. Chim. Acta*, 1977, **46**, 1.
24 T. Ziegler and A. Rauk, *Inorg. Chem.*, 1979, **18**, 1558.
25 E. J Baerends, V. Branchadell and M. Sodupe, *Chem. Phys. Lett.*, 1997, **265**, 481.
26 J. E. Huheey, E. A. Keiter and R. L. Keiter, *Inorganic Chemistry*: *Principles of Structure and Reactivity*, HarperCollins, New York, 4th edn., 1993, p. 421.
27 D. M. Hoffman, R. Hoffmann and C. R. Fisel, *J. Am. Chem. Soc.*, 1982, **104**, 3858.
28 N. Kaltsoyannis, unpublished work.
29 P. Mountford and D. Swallow, *J. Chem. Soc.*, *Chem. Commun.*, 1995, 2357.

Paper 8/07136E